

## GSA DATA REPOSITORY 2014202

### Stevensite in the modern thrombolites of Lake Clifton, Western Australia: A missing link in microbialite mineralization?

Robert V. Burne, Linda S. Moore, Andrew G. Christy, Ulrike Troitzsch, Penelope L. King, Anna M. Carnerup, and P. Joseph Hamilton.

### SAMPLE PREPARATION METHODS

Samples (Table DR1) were selected to represent the variety of thrombolite forms in Lake Clifton documented by Moore and Burne (1994).

**Table DR1: Samples Studied**

Sample Number	Depth (m)	Form	Locality	Location
85635773	1.5	Tabular	West of former UWA Field Station	32°49'9"S 115°40'44"E
85635776	2.5	Column	Deep Water Channel	32°50'29"S 115°41'19"E
86635073	1.5	Tabular	North of Tavern	32°47'1"S 115°39'59"E
86635078	2.2	Cone	South of Mt John	32°44'49"S 115°39'16"E
86635023	1.5	Tabular	North End	32°43'4"S 115°38'13"E
86635204	1.0	Dome	Western Shore opposite Mt John	32°44'51"S 115°38'34"E

All specimens except 85635773 were vacuum impregnated with epoxy resin using the method of Tratt and Burne (1982), then slabbed and polished by Malcolm Tratt (deceased) and Gary Bickford in the Baas Beeking Geobiological Laboratory. 25-mm-diameter discs were drilled from slabs and polished by Shane Paxton, and petrographic thin sections 30 µm in thickness were made by John Vickers at RSES. Polished sections and discs were carbon-coated for backscattered electron imaging and EDS, while broken fragments were mounted on aluminum stubs and platinum-coated for secondary electron imaging analysis by Joanne Lee at CAM, ANU. An unimpregnated thrombolite (No. 85635773) was sampled for XRD and IR analysis.

## Experimental Methods

### *SEM imaging*

Polished samples were carbon-coated, and imaged using backscattered electrons in the JEOL 6400 SEM and Hitachi 4300 Schottky FESEM at the Centre for Advanced Microscopy, ANU. Samples were degassed in a vacuum chamber prior to loading into the FESEM. Accelerating voltage was 15 kV.

### *EDS analysis*

The electron beam incidence on a sample generates X-rays, the energy spectrum of which is a function of the elements present and their proportions. For manually selected spot analyses, the spectra can be quantitatively resolved as a chemical composition and then related to known mineral compositions. For the data shown in Table DR2, samples were analysed on the JEOL 6400 SEM at the Centre for Advanced Microscopy, ANU, using Oxford Instruments Link ISIS quantification software.

Accelerating voltage was 15 kV, probe current was 1 nA (JEOL) and spectra were collected for 180 live seconds. Analytes and standards were albite (NaK, AlK), periclase (MgK), sanidine (KK),  $\text{CeP}_5\text{O}_{14}$  (PK), orpiment (SK), halite (ClK), diopside (CaK), rutile (TiK), rhodonite (MnK), hematite (FeK). Later imaging with phase identification by EDS was conducted on the Hitachi 4300 Schottky FESEM at 15 kV, 0.6 nA, using INCA quantification software.

### *QemSCAN Analysis*

During QemSCAN analysis (Pirrie et al., 2004) the sample is scanned automatically at a pre-determined point spacing of 2  $\mu\text{m}$  and using an accelerating voltage of 15 kV. The X-ray spectrum generated at each point is compared with a library of mineral spectra and the minerals or minerals present so identified.

### *XRD*

XRD analysis measures the intensity and angle of reflections consequent to monochromatic X-ray irradiation. This provides measures of lattice spacings and their changes after different treatments that are compared with standard spectra for mineral identification.

Powder X-ray diffraction of bulk and clay samples was carried out with a SIEMENS D501 Bragg-Brentano diffractometer (reflection geometry) equipped with a graphite monochromator and scintillation detector, using  $\text{CuK}_\alpha$  radiation. The corundum-spiked sample used for phase quantification was analysed with a SIEMENS D5005 Bragg-Brentano diffractometer (reflection geometry) equipped with a graphite monochromator and scintillation detector, using  $\text{CoK}_\alpha$  radiation.

**Table DR2. Representative EDS analyses of stevensite in thrombolites**

wt%	1	2	3	4	5	6	average
SiO <sub>2</sub>	33.35	36.10	33.22	31.74	33.98	34.07	33.74
Al <sub>2</sub> O <sub>3</sub>	1.40	0.30	-	0.40	-	-	0.37
FeO	0.06	-	0.07	0.64	0.41	0.18	0.23
MnO	0.00	0.02	0.09	-	0.10	0.07	0.05
MgO	17.18	16.24	15.23	15.38	15.44	17.39	16.04
CaO	1.21	1.34	1.76	1.20	1.49	1.22	1.37
SrO	-	-	0.17	0.20	0.05	0.40	0.14
Na <sub>2</sub> O	0.01	-	-	0.30	0.32	-	0.11
K <sub>2</sub> O	0.02	0.02	0.01	0.10	0.12	0.02	0.05
P <sub>2</sub> O <sub>5</sub>	-	0.02	0.08	0.06	-	0.12	0.05
SO <sub>3</sub>	1.05	0.65	0.54	0.58	1.52	0.91	0.88
Cl	0.07	-	0.02	0.44	0.43	0.03	0.17
-O $\equiv$ Cl	-0.02	-	-	-0.10	-0.10	-0.01	-0.04
TOTAL	54.33	54.78	51.22	50.94	53.76	54.53	53.26

Numbers of atoms, normalised to 11 oxygens after removal of Cl, S and P\*

Si	3.85	4.06	4.03	3.94	4.06	3.94	3.98
Al	0.19	0.04	-	0.06	-	0.02	0.05
Mg	2.95	2.72	2.75	2.85	2.75	2.99	2.84
Fe	0.01	-	0.01	0.07	0.04	0.02	0.02
Mn	-	-	0.01	-	0.01	0.01	-
$\Sigma$							
octa+tetrahedral	7.00	6.82	6.79	6.91	6.87	6.97	6.89
Ca	0.06	0.11	0.17	0.10	0.05	0.05	0.09
Na	-	-	-	-	-	-	-
K	-	-	-	0.02	0.02	-	0.01
Sr	-	-	0.01	0.01	-	0.03	0.01
$\Sigma$ interlayer	0.06	0.11	0.18	0.13	0.07	0.08	0.11

\*These components are likely to be present in impurity phases. Cl was removed as NaCl, S as CaSO<sub>4</sub> and P as Ca<sub>5</sub>(PO<sub>4</sub>)<sub>3</sub>OH before calculation of stoichiometry.

Note: Locations for samples analysed are: Samples 1, 2, 3, & 6 – tabular thrombolite sample 86635073, 1.5 m water depth, northeastern Lake Clifton. Samples 4 & 5 – conical thrombolite sample 86635078, 2.2 m water depth, northeastern Lake Clifton

Bulk samples were milled for 10 min in ethanol with a McCrone Micronizing Mill, and dried at 40°C. Samples were suspended on a side-packed sample holder, and analysed on the D501 from 2 to 70° 2 $\theta$ , at a step width of 0.02°, and a scan speed of 0.5° per minute, and on the D5005 from 4 to 84° 2 $\theta$ , at a step width of 0.02°, and a scan speed of 15 s per step.

Clay separation was performed by the settling method, and oriented samples prepared according to the Millipore Filter Transfer Method (Moore and Reynolds, 1997). Clay samples were analysed after Mg-saturation (scan range 2-42° 2 $\theta$ ), saturation with ethylene glycol (2-32° 2 $\theta$ ), and heating to 350°C (2-28° 2 $\theta$ ) and to 550°C (2-28° 2 $\theta$ ), all at a step width 0.02° and scan speed of 0.3°/min. The results were interpreted using the Bruker AXS software package *Diffractionplus* Eva 10 (2003) for identification, and *Siroquant V3* for quantification (using the bulk scan). Phase quantification of the bulk sample was undertaken by Rietveld analysis (Reitveld, 1969) after spiking with 20% corundum.

#### *Fourier Transform Infrared Spectroscopy*

The FTIR method utilises the absorption of infra-red light at specific wavelengths by different bonds between atoms and groups of atoms to identify from the absorption spectra the minerals that are present. Clay-rich powder from a Lake Clifton thrombolite was analyzed using Fourier Transform Infrared (IR) spectroscopy in the Research School of Earth Sciences, ANU. A bulk powder sample was prepared in a KBr disc and analyzed using a Bruker Tensor 27 spectrometer with a Globar source, KBr beamsplitter and DTGS detector from 5400 to 400 cm<sup>-1</sup>, 4cm<sup>-1</sup> resolution and 100 scans. Micro-analyses were made in transmission mode on powders suspended on a CaF<sub>2</sub> disc using a Hyperion microscope with a Globar source, KBr beamsplitter and MCT-A detector from 5400 to 600 cm<sup>-1</sup>, 4cm<sup>-1</sup> resolution and 300 scans. The results were compared with other published IR spectra (Figure DR1). Note that the variation in band intensity in the 800–1800 cm<sup>-1</sup> region is due to variations in crystallographic orientation of the sample, and those variations help to confirm some of the bands that appear as shoulders in the spectrum of the bulk sample. Spectral bands identified in the samples correlate well with those in the literature. Labels in the Figure and assignments are: *a*- 3680 cm<sup>-1</sup> structural (x)-OH vibrations; *b*- 3430 cm<sup>-1</sup> bulk sample structural and amorphous/adsorbed (x)-OH vibrations; *c*- 3380 cm<sup>-1</sup> micro-analysis structural (x)-OH vibrations; *d*- 1785 cm<sup>-1</sup> weak band likely related to the Si-O species overtones; *e*- 1635 cm<sup>-1</sup> structural H-O-H stretching; *f*- 1388 cm<sup>-1</sup> unknown band; *g*- 1050 cm<sup>-1</sup> shoulder related to the silicate structure; *h*- 1013 cm<sup>-1</sup> related to the silicate structure; *i*- 910 cm<sup>-1</sup> shoulder related to the silicate structure.

#### *X-ray computed microtomography (micro-CT)*

An X-ray tomogram was acquired of the Lake Clifton sample No. 85635773 (Figures DR2, DR3) using the ANU micro-CT facility (Sakellariou et al., 2004). The X-ray source (X-Tek RTR-UF225) was operated at 120 kV and 120  $\mu$ A, which produces a polychromatic cone beam. The lower energy X-rays were removed by an aluminium filter and the projection data was

collected using a digital X-ray flat panel detector (2048<sup>2</sup> pixels, PerkinElmer). 2880 radiographs were collected over 17 h using a circular sample trajectory (one revolution of 360°) and the data was reconstructed to produce a tomogram with voxel size of 80 µm. To explore the 3D pore structure in the thrombolite the data was visualized using DRISHTI (2013) software.

## References

DRISHTI, 2013, Volume exploration and presentation tool: <http://sf.anu.edu.au/Vizlab/drishti/> (January 2014).

Elton, N. J., Hooper, J. J. & Holyer, V. A. D., 1997, An occurrence of stevensite and kerolite in the Devonian Crousa gabbro at Dean Quarry, The Lizard, Cornwall, England: *Clay Minerals*, v. 32(2), p. 241-252.

Faust, G. T., Hathaway, J. C. & Millot, G., 1959, A restudy of stevensite and allied minerals: *American Mineralogist*, v. 44, p. 342-370.

Moore, D. M. & Reynolds, R.C., 1997, *X-ray Diffraction and the Identification and Analysis of Clay Minerals*, 2<sup>nd</sup> ed, Oxford, Oxford University Press, Oxford, 378 pp.

Moore, L.S. & Burne, R.V., 1994, The modern thrombolites of Lake Clifton, Western Australia. In Bertrand Sarfati, J. & Monty C. L., Eds. *Phanerozoic Stromatolites II*, Dordrecht, Kluwer Academic, p. 3-29.

Pirrie, D., Butcher, A.R., Power, M.R., Gottlieb, P., & Miller, G.L. (2004) Rapid quantitative mineral and phase analysis using automated scanning electron microscopy (QemSCAN); potential applications in forensic geoscience. In: *Forensic Geoscience; Principles, Techniques and Applications*, Geological Society Special Publication, v. 232, p 123-136.

Rietveld, H. M., 1969, A profile refinement method for nuclear and magnetic structures: *Journal of Applied Crystallography*, v. 2 (2), p. 65–71.

Sakellariou, A., Sawkins, T.J., Senden, T.J. & Limaye, A., 2004, X-ray tomography for mesoscale physics applications: *Physica A*, v. 339, p. 152-158.

de Santiago Buey, C., Barrios, M. S., Romero, E. G. & Montoya, M. D., 2000, Mg-rich smectite “precursor” phase in the Tagus Basin, Spain: *Clays and Clay Minerals*, v. 48(3), p.366-373.

Tratt, M.H. & Burne, R.V., 1982, Impregnation of Unconsolidated sediment samples using a large vacuum chamber. *BMR Journal of Australian Geology and Geophysics*, v. 7, p. 225-226.

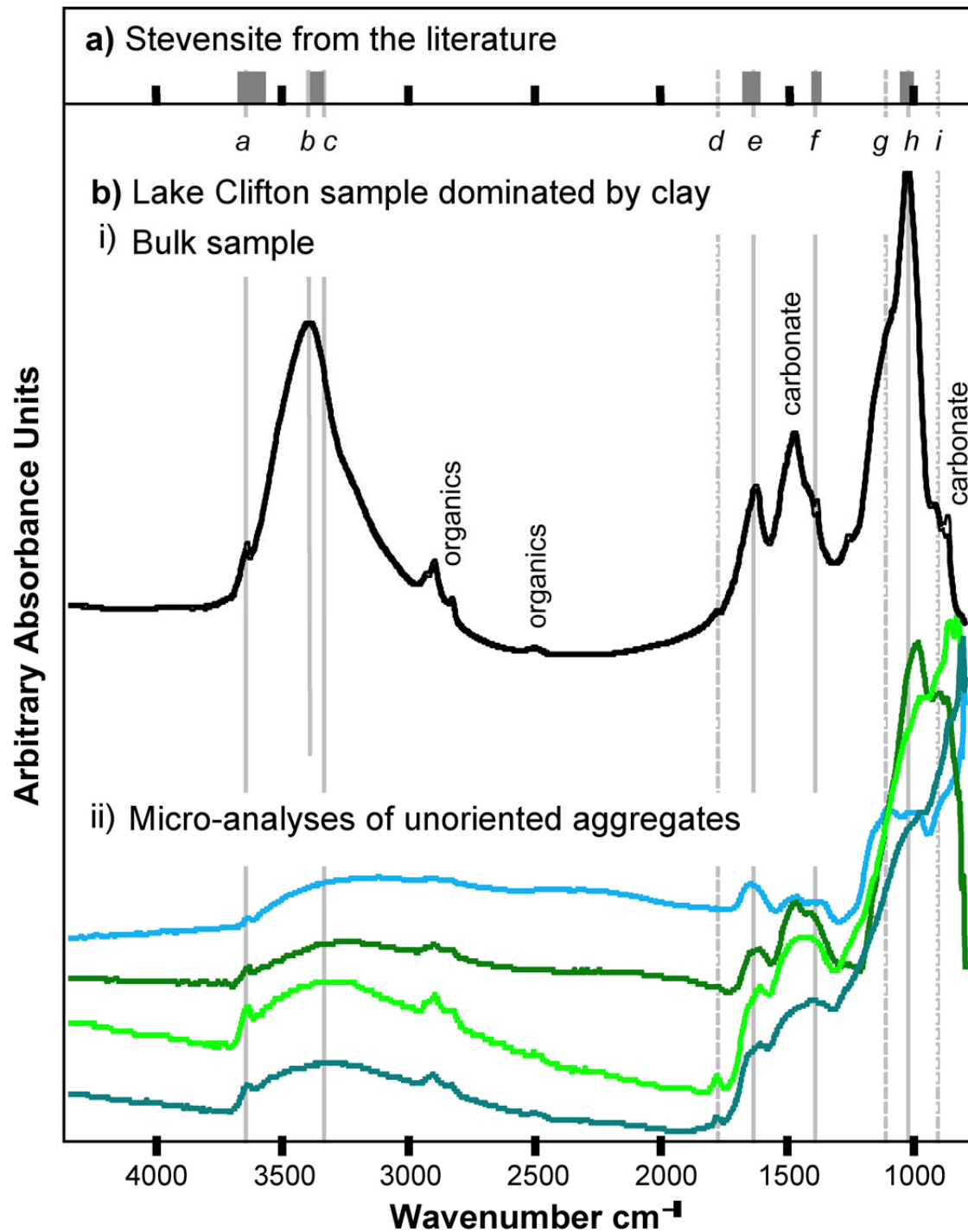


**Figure DR1.** IR Analyses. (a) Stevensite bands from de Santiago Buey et al. (2000), Faust et al. (1959) omitting carbonate bands), Elton et al. (1997). (b) Mid-IR spectra for samples from Lake Clifton that were dominated by clay, showing (i) a bulk sample measured in a KBr disc and (ii) microanalyses of clay-dominant aggregates suspended on a  $\text{CaF}_2$  substrate.

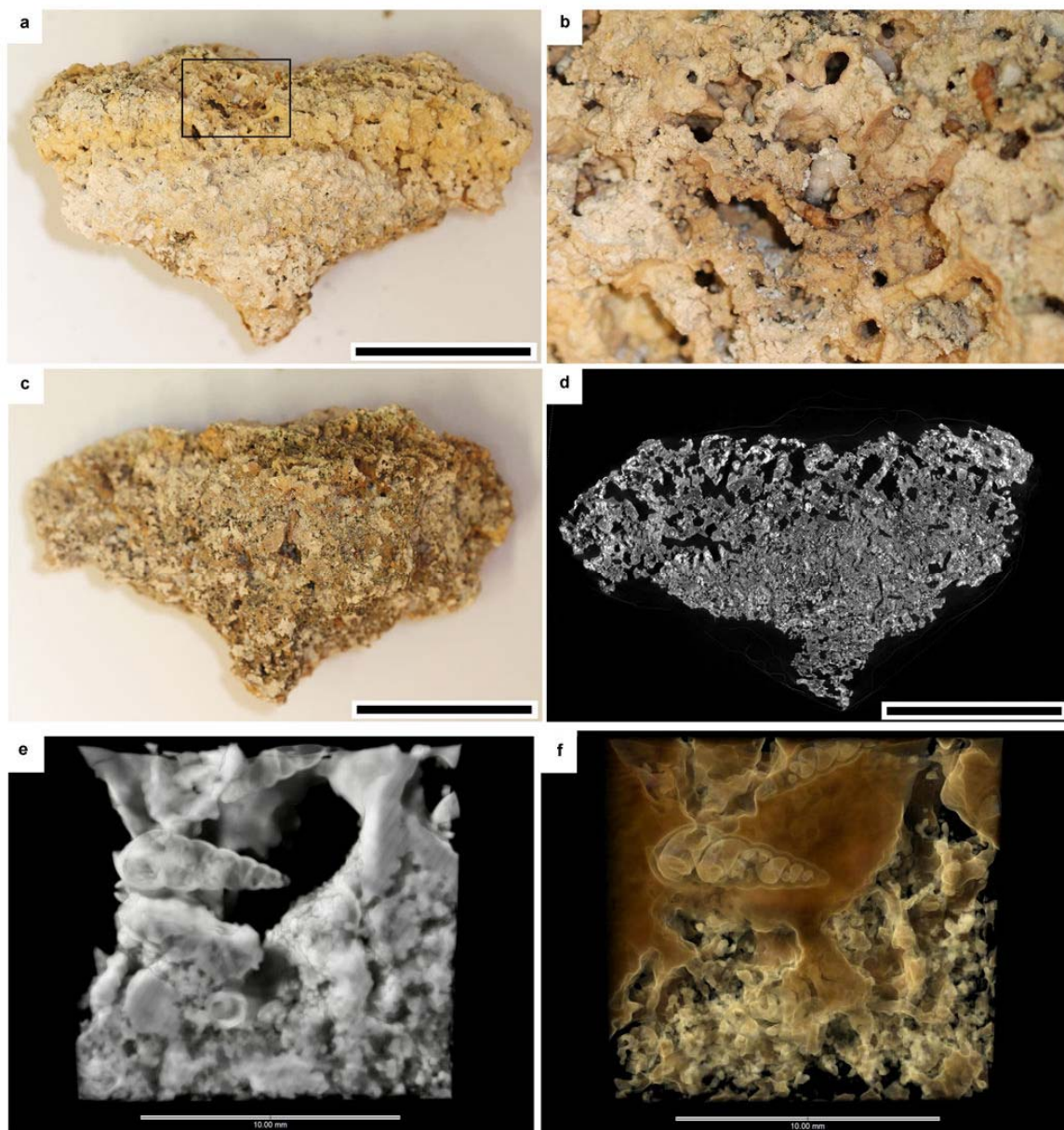


**Figure DR2.** (a,b,c) Photographs and (d) a slice from the 3D X-ray tomogram of a poorly lithified thrombolite (sample 85635773) from ~ 1.5 m water depth adjacent to the former UWA Field Station, eastern Lake Clifton. Photograph (b) is a magnification of the area indicated by the black box in image (a). Photograph (c) is the reverse side of sample to that in (a). Note the large cavities present at the surface of the thrombolite (b, d). The micro-CT image (d) displays contrast dependent on mineral density and porosity, with the brighter areas presumably representing calcium carbonate dominated regions. Note that here is no significant evidence for widespread burrowing or boring of the structure. All scale bars are 5 cm. (e,f). Micro-CT images of a cavity within sample 85635773. Note gastropod shell within a primary cavity. (e) shows solid material, (f) shows pore space. Scale bars are 10 mm.



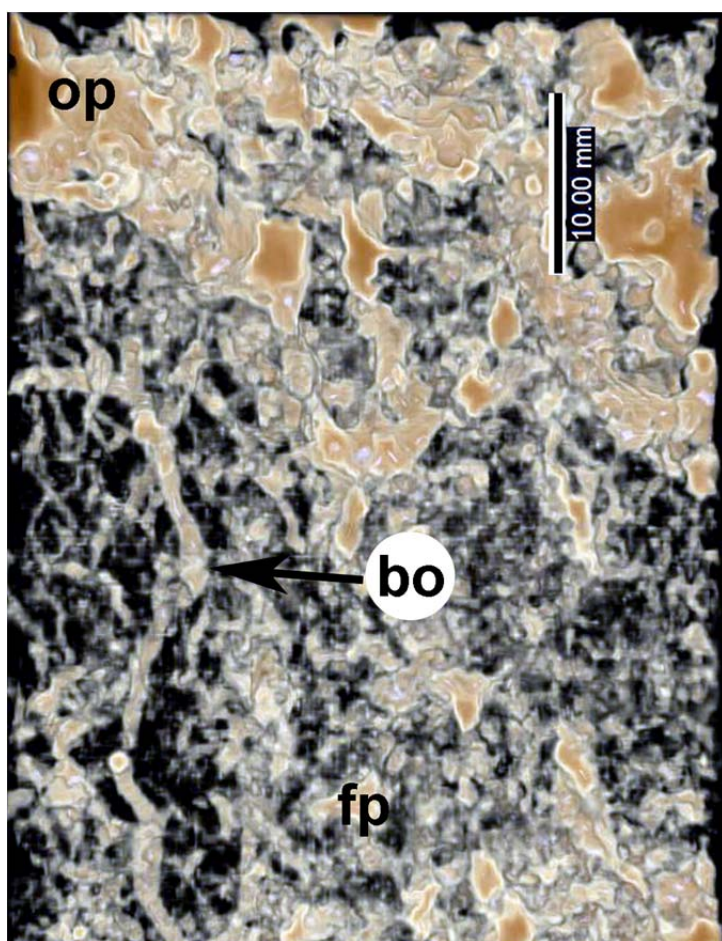


**Figure DR3.** Micro-CT image of the 3-dimensional distribution of porosity in sample 85635773. Note empty cavities near surface of the structure (op), vertical tubular borings (bo), and partially filled cavities lower in the structure (fp). Scale bar 10 mm.